



Volume XXIV 2021

ISSUE no.1

MBNA Publishing House Constanta 2021



Scientific Bulletin of Naval Academy

SBNA PAPER • **OPEN ACCESS**

Dynamic simulation of a reciprocating compressor in LMS Amesim program

To cite this article: Ion PANA, Scientific Bulletin of Naval Academy, Vol. XXIV 2021, pg.29-40.

Submitted: 27.02.2021

Revised: 15.06.2021

Accepted: 22.07.2021

Available online at www.anmb.ro

ISSN: 2392-8956; ISSN-L: 1454-864X

doi: 10.21279/1454-864X-21-I1-003

SBNA© 2021. This work is licensed under the CC BY-NC-SA 4.0 License

Dynamic simulation of a reciprocating compressor in LMS Amesim program

I Pana

Associate professor, Petroleum & Gas University, Ploiesti, Romania
E-mail: ion.pana@upg-ploiesti.ro

Abstract. The evolution of calculation programs currently allows the modelling of engineering systems with a high degree of accuracy, reducing the simplifying assumptions used in the construction of models. The paper presents a combined model of a pulsation damping system and a cooling system of a reciprocating compressor. The numerical simulation uses the LMS Amesim program, the academic license offered free of charge by Siemens to teachers and students. The model with a large number of tracked variables allows the analysis of adjustments and the effects of changes to the conditions in the compression system. They are considered: the drive mechanism, the structure of the compression cylinders, the influence of the dead space, the compressor valves, the gas composition, the suction and discharge pipelines, the anti-pulsation bottles, the heat exchangers for the gas cooling. They are indicated the modalities of action regarding the fulfilment of the conditions mentioned in the standards regarding the pressure variation, the damping of the pressure waves, the reduction of the energy losses and an efficient cooling.

1. Bibliographic analysis

For the installations where reciprocating piston compressors are used, a detailed dynamic design is usually required to ensure a successful installation. The American Petroleum Institute (API) Pulse Control Section 618 [1] is the most commonly used for these types of studies, [2].

Atkins in [3], presents some of the best engineering practices for pulsation and vibration control for the dynamic reciprocating equipment used in the natural gas industry. Ghanbariannaenianalyzed the vibration problems in plants with reciprocating machinery and described some procedures for calculating the pressure pulsation as well as detailed information to help understanding the causes of acoustically induced pulsation shaking forces. It was mentioned that acoustical and mechanical study shall indicate the necessary improvements to achieve the target values of pulsation and vibration for safety and reliability [4].

Sometimes [5] in order to obtain an efficient pulsation reduction system, it is necessary to use two series of anti-pulsation bottles. Although apparently this method is more expensive, compared to the side effects of the one-bottle method, the proposed solution becomes economical and safe. Shejal in the paper [6] properly analyzed the vibrations of the compressor pipes, using Pulsim and Ansys software. The accuracy of the analytical solution is validated through experimental results using Brule &Kajer analyzer for the measuring of the compressor pipelines.

Article [7] based on the finite element analysis and experimental determinations, identified the vibration modes of the compressor determined by the position of moving parts and fasteners. Jia in [8] presents the results of testing and associated analyzes to suppress pressure pulsations in the valve chamber and cylinder nozzle for a reciprocating compressor with a control method based on the

Helmholtz resonator. A three-dimensional acoustic model of the gas pulsation was established using the finite element method (FEM) for the compressor and the discharge pipe system with and without resonator. The results showed that the amplitude with which the presence in the valve chamber pulses was reduced by 40.4% the installation of the resonator. Almasi presented a model for the study of pulsation and pressure force generated into the equipment and pipelines in [9]. In order to calculate the velocity and the pressure at every point, in time, a transient one dimensional NavierStokes model was used. The information obtained from the pulsation simulation method presented allows the design of a gas transmission network that ensures the optimal solution for reducing of the pulsations.

In the paper [10] Okasha used the two-port theory to model a pipeline network, where the network can be divided into several series elements, each described by a transfer matrix. A pilot plane equipped with a reciprocating compressor, pipes, bends, and a vessel were constructed. Two cases are investigated; one with a long pipe, the other with a pulsation suppression device designed according to the API-618 standard. The comparison shows good agreement between the measured dynamic pressures and the predicted ones using 1D propagation models. The pressure variation can be effectively attenuated over the entire pipeline network at different compressor speeds, when a perforated cross-flow tube is installed downstream of the anti-pulsation bottle. The pulsation damping performance is better for a longer tube with a lower perforation rate, while the hole diameter has little influence on the pulsation attenuation of the piping system [11]. Maximum recommended pressure drop values in the pulsation dampeners and suppression devices is 1 % of the pressure [12].

Liu analyzed the influence of a conical cylinder discharge nozzle on pressure pulsations in a piping system with high-speed reciprocating compressor [13]. Pressure fluctuations can be effectively attenuated in the pipeline system at variable compressor speeds and pressures. The same author in [14] presented a nonlinear mathematical model used to simulate the pulsating flow in a reciprocating compressor piping system on a perforated tube device. An investigation was carried out into the effects of the geometric parameters and operating conditions of the compressor. A longer perforated tube achieved better damping performance, while the hole diameter had a reduced effect on pressure pulsations. The damping capacity was less sensitive to the average pressure in the pipes than to the operating speed of the compressor.

There are many more forces associated with an alternate separable compressor, other than pulsations, which can lead to unacceptable vibrations. Fifer in the paper [15] discusses the main sources of forces and presents a mechanical guide that will help avoid mechanical resonance due to these sources. He emphasizes that when conducting acoustic studies, companies required in addition and mechanical analysis. There is currently no specific mechanical guidance in API Standard 618. It focuses only on the effects of pulsations. The article [16] compares two methods for thermal modeling of a reciprocating compressor. The first model is based on parametric relations that incorporate infinitesimal displacements depending on the movement of the piston. The second model includes the analysis and modeling of the compressor by applying the method of neural networks. The inlet variables are: suction pressure, suction temperature, discharge pressure and compressor rotation speed. The output parameters are: flow rate, discharge temperature and energy consumption. Computer simulations show that the average relative errors are below $\pm 10\%$ in the physical model and below $\pm 1\%$ when using artificial neural networks. Yinshui [17] evaluates the volumetric efficiency of each stage (the compressor has 4 stages) of a miniature compressor with an insufficient cooling conditions between stages, by numerical simulation. The results show that the volumetric efficiency of all steps is reduced by values between 1.5 - 2.5% as the suction temperature increases by 10°C . If the suction temperatures in steps 2,3 and 4 increase to values of $70 - 120^\circ\text{C}$ the valves flutter severely, indicating that the valves have little use in these operating conditions. A test stand was developed to study the thermal conditions of long stroke piston compressors [18,19]. In the calculation techniques known for calculating of the heat exchange processes, for reciprocating compressors, the empirical dependencies obtained depend essentially on the stroke / diameter ratio and the duration of the operating cycle. The article recommends the using the experimental method for better accuracy.

One of the main factors affecting the isentropic efficiency of the reciprocating compressor is the heat transfer inside the cylinder [20]. An analysis of heat transfer can be done using numerical models or analytical correlations developed mainly from the approaches used in the internal combustion engines. Their accuracy is not fully verified due to the complicated experimental configuration. Various analytical correlations for different compressor and fluid settings were compared in the paper. The CoolProp library was used in the code to obtain the common properties of coolants fluids and gases. A comparison was made using the internal code developed in Matlab, based on the first principle of thermodynamics.

The duty cycle of a reciprocating compressor is characterized by the generation of heat, mainly due to the phenomena of compression and friction. The main consequences are a reduction in volumetric efficiency and an increase in the exhaust temperature. The current API618 regulations for reciprocating compressors require a cylinder cooling system. Therefore, a proper design of the cooling circuit is necessary to get the best results. In paper [21], a conjugate heat transfer analysis on a cylinder of a water-cooled double-acting reciprocating compressor is presented. Simulations were performed with the ANSYS CFX software package by means of a 3-D steady-state Reynolds Averaged Navier-Stokes (RANS) analysis. The evaluation by numerical methodology is completed with an investigation that includes the influence of wall roughness and buoyancy effects.

The suction process for reciprocating compressors is strongly affected by the valve dynamics and the pulsating flow through the pulsation damper on the suction. The paper [22] describes a simplified model of computational fluid dynamics (CFD), simulating the flow through the pulsation damper, the suction valve and a small region inside the cylinder. The proposed method is applied to predict the suction process of a reciprocating compressor and its suitability is compared to a complex model over time in terms of accuracy, calculation cost and use. The model returns predictions in close agreement with those obtained in a more comprehensive way and on a more complicated and expensive calculation model. Only a small region of the cylinder is included in the simplified model solution area and this considerably reduces both the network preparation effort and the simulation calculation cost. The play and geometry of the cylinder can be easily adjusted in the simplified model. The complete CFD model requires a new calculation grid in case of any change in the cylinder geometry.

An integrated simulation model has been developed and implemented for reciprocating compressors in [23]. Compressor flow and isentropic efficiency were calculated. The overall performance of the compressor was simulated as in a standard calorimetric test system. The analysis is focused on the compressor, the simulation model includes heat transfer and flow resistance in the compressor components, the effect of the re-expansion volume, leaks through the gap between the piston and the cylinder, loss of power in the bearing, loss of friction of the piston, losses of oil flow and valve dynamics. Some empirical factors have been used in the model, so that the prediction can be more accurate with little test data. A program module was developed and included in the program for bearing analysis. Some useful data for component design were obtained.

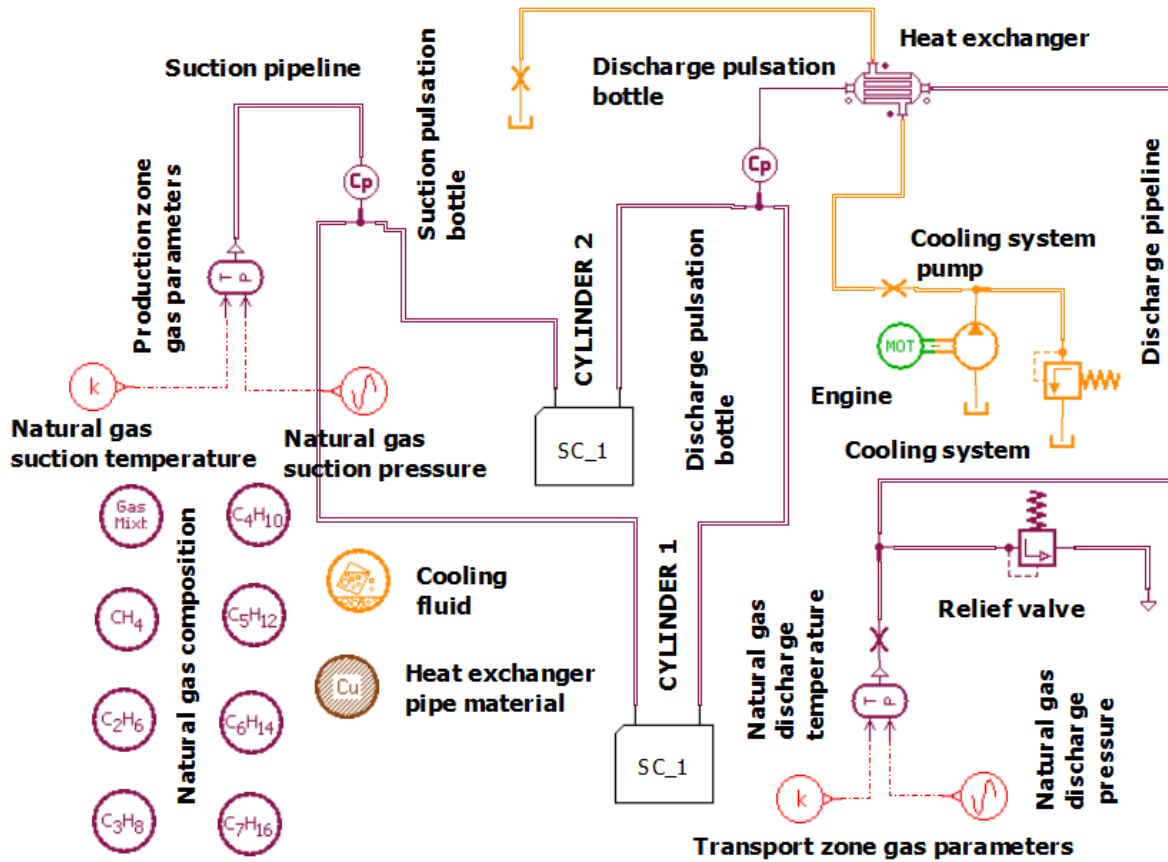
2. Dynamic simulation of a reciprocating compressor in LMS Amesim

2.1. Sizing anti-pulsation bottles

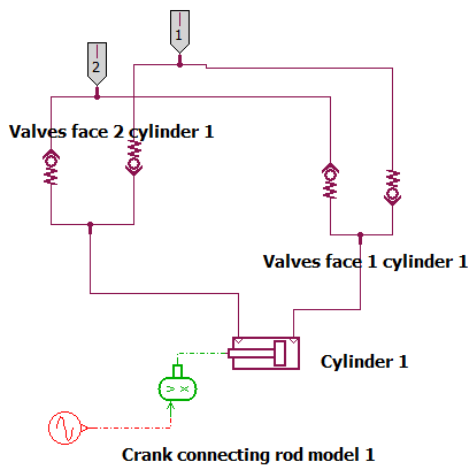
Anti-pulsating bottles are mounted at the inlet and outlet of / from the compressor cylinders to even out the gas parameters. This ensures stable working conditions in the compressor cylinders and eliminates / reduces vibrations. For the calculation of the pre-sizing of the anti-pulsating bottles it is necessary to know the compressor displacement (volume of gas aspirated for a double stroke)[1]:

$$P_{d1} = S_t \cdot i \cdot \frac{\pi(2D^2 - d^2)}{4}, \quad (1)$$

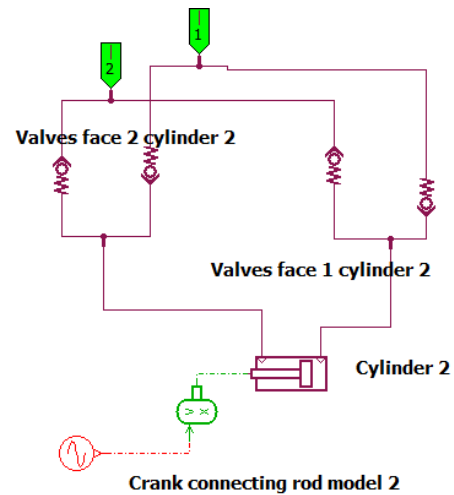
where S_t is the stroke length, D piston diameter; d rod diameter and i is the number of compressor cylinders to be manifolded in the surge volume, in cubic meters per revolution. The minimum volume of the anti – pulsation bottle on the suction V_g is determined by the relation:



a



b



c

Figure 1. Model of the anti-pulsation bottles in the LMS Amesim program: a. model of the compression and pulsation bottles, cylinders 1 and 2; b. using of the cylinder sub model for cylinder 1; c. the sub model of cylinder 2.

$$V_s = 8.1P_{d1}^4 \sqrt{\frac{kT_s}{M}}, \quad (2)$$

where k is the adiabatic exponent; T_s temperature of the gas on the suction pipe in K; M molar mass of the gas [1]. The following conditions are imposed:

$$V_s \geq V_d \text{ \textit{ \textless} } V_s \geq 0.028m^3 \quad (3)$$

The minimum volume of the anti – pulsation bottle on the discharge V_d is determined by the relation:

$$V_d = 1.6 \frac{V_s}{r^{1/k}}, \quad (4)$$

where r is the compression ratio on the stage on which the cylinder is mounted. The molar mass of the mixture M kg / kmolis determined by the relationship:

$$M = \sum_{i=1}^n y_i \cdot M_i \quad (5)$$

where y_i are the molar fractions of the components of the mixture, M_i are their molar masses and n the number of gas components. For the adiabatic exponent k the relation (6) is used:

$$k = 1,9637 \cdot M^a + \frac{t - 10}{27,7} (1,9927 \cdot M^b - 1,9637 \cdot M^a) \quad (6)$$

where t is the average temperature of the gas in the cylinder, ° C; a, b - dimensionless coefficients: $a = -0.1463$; $b = -0.1543$, [24]. The unfiltered peak-to-peak pulsation level at the compressor cylinder flange, is indicated by the relation (7)[1]. The recommendation if for the design approaches 1, 2, and 3:

$$P_{cf} = \min(3r; 7) [\%]. \quad (7)$$

For the design approach 1, allowable pulsations at the pipeline side of the anti-pulsation bottle shall not exceed the value calculated from equation (8). The maximum allowable peak-to-peak pulsation level at any discrete frequency, as a percentage of average absolute pressure [1] is:

$$\Delta p \% = \frac{4.1}{p_n^{1/3}}, \quad (8)$$

where p_n is the average absolute pipeline pressure, in bar.

2.2. Checking the anti-pulsation bottles in the LMS Amesim program

In order to check the sizing of the anti-pulsating bottles (see the criteria set out in point 2.1), a model was made in LMS Amesim program, fig. 1.a. For the study, two cylinders of a piston compressor were considered, that take natural gas from a production group and transmit it to the transport network. The compressor flow (150,000 Scm) was divided between the two cylinders to reduce their dimensional elements. The model contains the following elements:

- Suction network parameters: temperature (288 K) and pressure (4 barA); parameters of the discharge network: temperature (288 K) and pressure (12 barA); the pressure can be changed according to an imposed law of variation/ experimental values.
- Anti-pulsation bottles C_p shaped like pneumatic chambers (suction/discharge bottle volume are $V_s=506$ l, $V_d=359$ l relations (2) and (4))
- Suction pipeline (length = 5 m, internal diameter $D = 300$ mm); discharge pipeline (length = 100 m, internal diameter $D = 200$ mm). Each pipeline has 6 segment, with different gas parameters, fig. 4.j.
- Suction and discharge valves of the compressor cylinders (flow area 7854 mm², pressure drop 0.02 barg/ (Smc/s)).
- Compressor cylinders and crank connecting rod system model, the cranks are shifted by 90 degrees, grouped in the sub models for cylinders fig. 1.b-c.
- The gas mixture block has been added which allows the precise introduction of the natural gas composition, fig. 6 a,i,j. For cylinders the geometric elements are introduced, fig. 2. The phase difference between the cylinders can be observed. The reduction of the pressure variation in the area of the transport pipeline is achieved with the device formed by two series vessels, according

to fig. 3 and joined by a shock tube. Equation (9) is used to calculate the filter frequency f_r of an ideal filter with no piping attached.

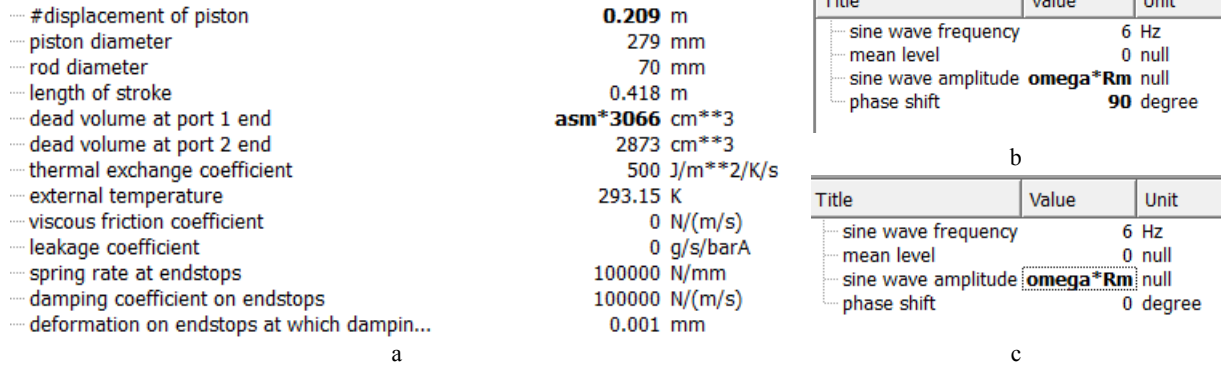


Figure 1. Cylinder characteristics: a. introduction of the geometric elements of cylinder 1 and cylinder 2 in the section Global parameters; b. the crank connecting rod mechanism, cylinder 1; c. crank connecting rod mechanism, cylinder 2.

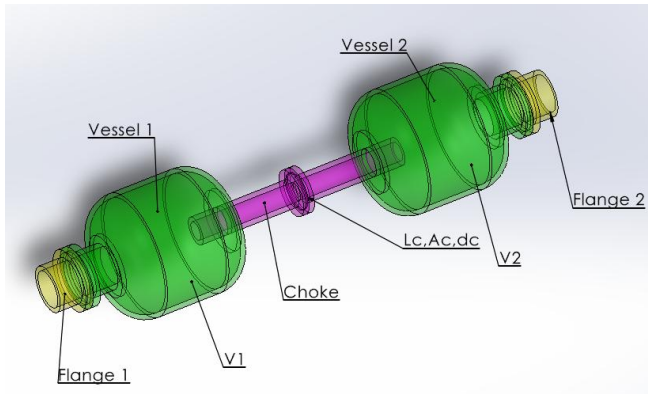


Figure 3. Filter type volume - choke- volume.

$$f_r = \frac{c}{2\pi} \sqrt{\frac{A_c}{L_{c1}} \left(\frac{1}{V_1} + \frac{1}{V_2} \right)} \quad (9)$$

$$L_{c1} = L_c + 0.6d_c \quad (10)$$

where f_r resonance frequency; c speed of sound in gas; A_c area of choke tube; L_c length of choke tube; d_c choke internal diameter; V_1 volume of primary bottle; V_2 volume of secondary bottle. *At frequencies above its characteristic resonance frequency f_r transmitted pulsation levels drop off rapidly.* The frequencies that can be transmitted to the pipeline are:

$$f_i = \frac{i \cdot n}{60}, \quad (11)$$

where: n machine speed, in rpm; i the integer 1,2,3 ... that corresponds to the fundamental frequency and harmonics of machine speed. To calculate the natural frequency of a pipeline with rigid supports we used the following formula:

$$f_n = \frac{11.2}{\pi} \sqrt{\frac{E \cdot I}{m_l \cdot L^4}}, \quad (12)$$

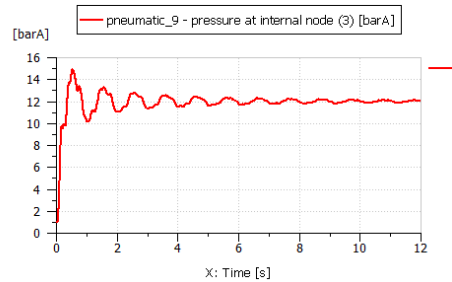
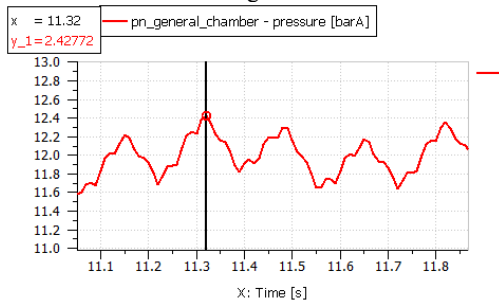
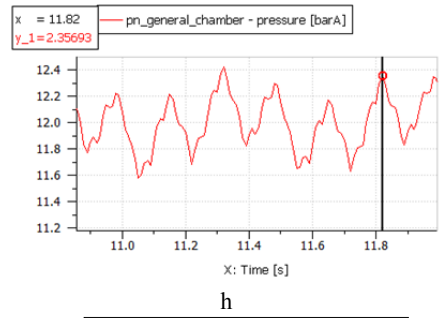
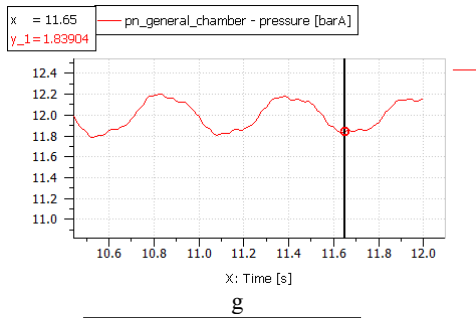
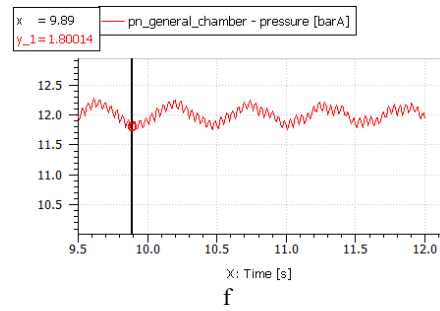
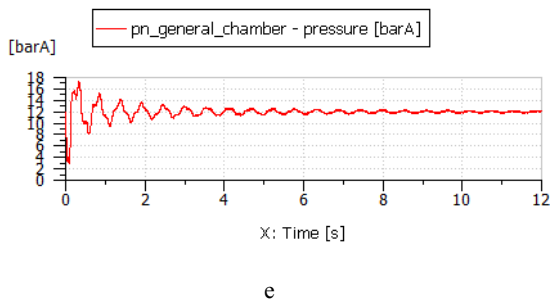
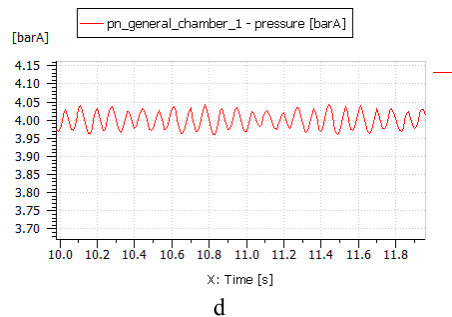
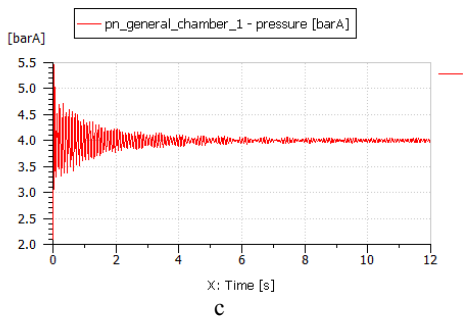
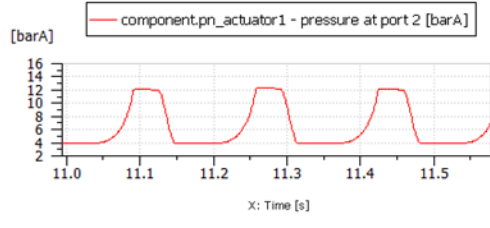
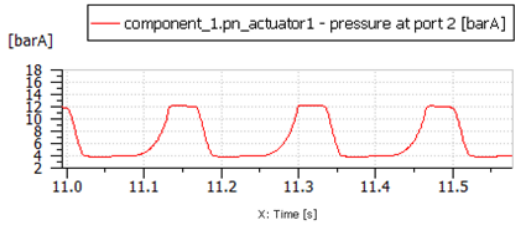
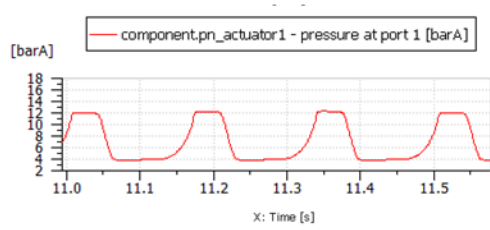
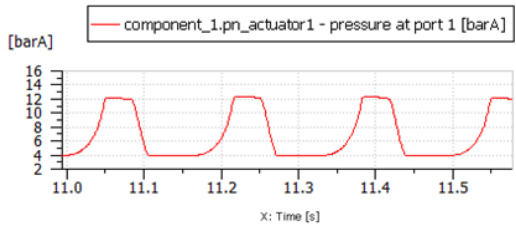


Figure 4. Pressure variations: a. (top –down) head end cylinder 1, crank end cylinder 1, in the active chambers of the compressor cylinder (the compressor has a single stage and two cylinders); b. (top –down) head end cylinder 2, crank end cylinder 2; c. suction bottle; d. suction bottle detail; e. discharge bottle; f. discharge bottle detail speed 360 rpm; g. discharge bottle (detail) speed 60 rpm; h. discharge bottle (detail) speed 360 rpm without suction valve head end cylinder 1; i. discharge bottle (detail) speed 360 rpm, dead space doubled (24 %); j. pressure variation on discharge pipeline in the section between segment 2 and 3 (pipeline has 6 segments).

where: f_n is the natural frequency of the pipe; E Young's modulus of elasticity (200GPa or 30E6psi for steel); I 4th polar moment of inertia for the pipe $\frac{\pi}{64}(D_e^4 - D_i^4)$ with D_e / D_i external /internal diameter of the pipeline; m_l mass per unit length of the pipe (including the mass of the gas)kg/m; L distance between pipeline supports. The excitations with frequencies f can disturb the pipeline, supports and equipment on it. An efficient sizing condition of the filter can be:

$$1.2f_r < f_i \text{ and } 1.2f_r < f_n \quad (13)$$

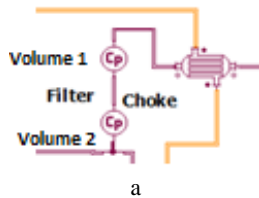
Inequalities (13) can be easily met by choosing a longer or smaller diameter of the choke. This means a higher pressure drop on the filter and a systematic energy loss at high gas volumes. The solution can be selective if we do not let frequencies higher than the natural frequency of the pipe and the equipment mounted on it pass. If possible we can go without a filter. Condition (13) is conservative. Following the modeling, you can see the diagrams of pressure variation in the pneumatic chambers. The suction, compression, evacuation and expansion of the gas are very well observed, see fig. 4,a-b.

Table 1. Discharge filter simulation results.

V_1	V_2	d_c	A_c	L_c	c	f_r	$\Delta p_{c1}/p_{c2}/\Delta p_s/\Delta p_a$
m^3	m^3	m	m^2	m	m/s	Hz	bar
0.359	0.359	0.03	0.000707	0.3	446	8.13	0.04/0.15/0.22/0.13
0.359	0.359	0.03	0.000707	0.55	446	6.00	0.02/0.16/0.42/0.13
0.359	0.359	0.03	0.000707	1	446	4.45	0.02/0.13/0.75/0.13
0.359	0.359	0.04	0.001256	2	446	4.16	0.03/0.15/0.37/0.13
0.359	0.359	0.05	0.001962	2	446	5.21	0.04/0.14/0.12/0.13

$\Delta p_a = 1.67(r - 1)/r$ acceptable pressure drop, API 618

For thenumerical example from fig. 4 c-d at suction, the pressure in the anti-pulsating bottle varies from 3.96 bar to 4.04 bar. At the flange from the pipeline ecuation (8) the permissible pressure variation is $\frac{4.1}{4^{1/3}} = 2.59\%$, namely $4 \frac{2.59}{100} = 0.1$ bar. The pressure variation (fig. 3.d) is $4.04 - 3.96 = 0.08$ bar, below the imposed limit. At the compressor flange equation (7) the allowed pressure variation is $\min(3 \cdot \frac{12}{4}; 7)$ namely $4 \frac{7}{100} = 0.28$ bar.



Name	Title	Expression	Default Result S	Value
p1	choke inlet pr...	(p1@pneumat...	ref	12.2484
p2	choke outlet p...	(p2@pneumat...	ref	12.0075
dp	choke pressur...	p1-p2	ref	0.24095

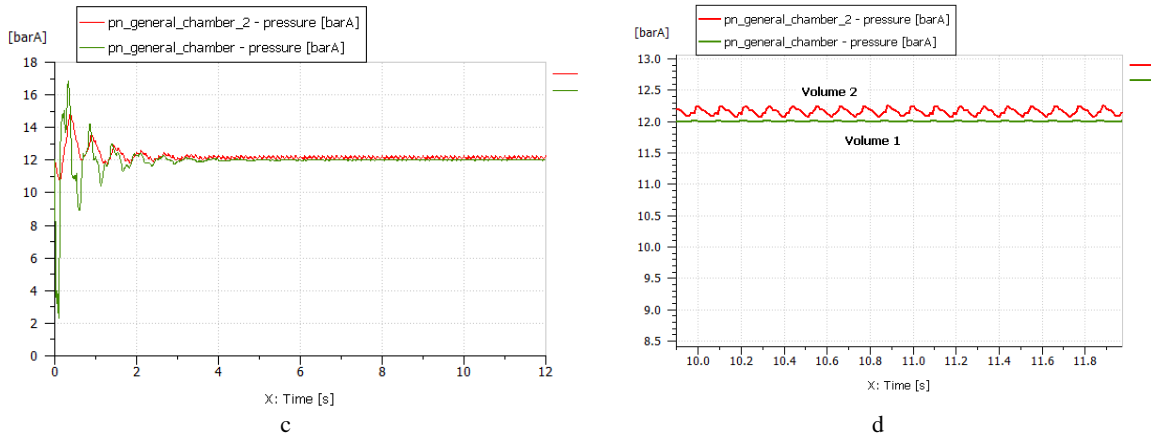


Figure 5. Using an acoustic filter: a. model modification on the discharge end; b. pressure drop on choke tub – in the post processing section; c. pressure variation in the volume 1 and volume 2; d. pressure variation in the volume 1 and 2 (detail).

The pressure variation (fig. 4.d) is $4.04 - 3.96 = 0.08$ bar, below the imposed limit of 0.28 bar. Regarding the variation of the pressure in the anti-pulsating cylinders on discharge (fig. 4.e-f) the pressure varies from 11.75 bar to 12.25 bar.

At the flange from the pipeline side (8) the allowed variation of the pressure is $\frac{4.1}{12^{1/3}} = 1.80\%$ ie $12 \frac{1.80}{100} = 0.22$ bar. The maximum pressure variation (fig. 4.f) is $12.25 - 11.75 = 0.5$ bar, so the maximum permissible limit is exceeded. The bottle must be resized or we can use a filter that also has the effect of cutting vibrations over a certain threshold.

At the compressor flange (7) the allowed pressure variation is $\min\left(3 \cdot \frac{12}{4}; 7\right) \cdot \frac{7}{100} = 0.84$ bar. The maximum pressure variation (fig. 4.f) is $12.25 - 11.75 = 0.5$ bar below the imposed limit of 0.84 bar.

If the crank shaft speed is lower the shape of pressure variation is different, fig. 4.g (for 60 rpm). The elimination of a suction valve fig. 4.h increase the pressure variation (for 360 rpm, 0.80 bar peak to peak). The increase of the dead space (24 % of displacement) generates a greater pressure variation, fig. 4.i (0.79 bar peak to peak).

The solution with the use of a filter involves the modification of the system from fig. 1.a, according to fig. 5.a. The shock tube causes a pressure drop between the two filter chambers, fig. 5.b and changes the shape and pressure values in the two chambers. At the outlet of the filter the pressure is almost constant, fig. 5.d. With the filter, the pressure variation at the pipeline flange is 0.03 bar, so the value is below the imposed limit of 0.22 bar.

Based on the values in the Table 1 (Δp_{c1} , Δp_{c2} pressure variation peak to peak in the volume 1 and 2; Δp_s pressure drop in choke; Δp_a acceptable pressure drop) it can be seen that in choke we have a pressure drop of 0.22 bar and a frequency of $f_r = 8.13$ Hz. The disturbing signal is 6 Hz. So the disturbing signal can pass through the filter. Increasing the length of the tube to 1 m, the disturbing signal of 6 Hz no longer passes through the filter (cut frequency is 4.45 Hz). This aspect is favorable because it prevents the pipeline and equipment destruction by vibration propagation. Under these conditions the pressure drop is higher 0.75 bar compared to 0.22 bar, which leads to additional energy consumption. So the negative aspect is connected with the pressure drop. We have a pressure drop on the choke of 0.75 bar. In fact, compressor will work at 12.75 barA (the average value) and for the value of flow of 150,000 Scm per day this means a power of 107.303 kW (with an acoustic filter) compared with 113.683 kW (in absence of the acoustic filter). In a year the additional power is 45,936 kWh (300 working days/year).

Title	Value	Unit
index for gas mixture	11	
number of species	10	
index of gas 1	1	
index of gas 2	2	
index of gas 3	3	
index of gas 4	4	
index of gas 5	5	
index of gas 6	6	
index of gas 7	7	
index of gas 8	8	
index of gas 9	9	
index of gas 10	10	
mass content of gas 1	0.908409	null
mass content of gas 2	0.035101	null
mass content of gas 3	0.016793	null
mass content of gas 4	0.003866	null
mass content of gas 5	0.005338	null
mass content of gas 6	0.001782	null
mass content of gas 7	0.00356	null
mass content of gas 8	0.020776	null
mass content of gas 9	0.001864	null
mass content of gas 10	0.0025	null

a

Title	Value	Unit
index of thermal hydra...	1	
pump displacement	450	cc/rev
typical speed of pump	1000	rev/min

c

Title	Value
index of thermal hydraulic fluid	1
fluid model	simple: database
simple fluid model database	pure water
cavitation / aeration model	none
Fluid temperature computation	none
assumption level	full energy balance (thermal-hydraulics)

e

g

Title	Value	Unit
@ pressure (absolute)...	1.013	barA
@ temperature at port 1	20	degC
@ temperature at port 2	20	degC
@ pressure at port 2	1.013	barA
@ pressure (absolute)...	1.013	barA
@ temperature at port 3	20	degC
@ temperature at port 4	20	degC
@ pressure at port 4	1.013	barA
@ wall temperature (3...	20	degC
@ wall temperature (1...	20	degC
@ energy stored in the...	0	J
liquid type index	1	
gas type index	1	
solid type index	1	
heat exchanger length	L	mm
heat exchanger diameter	D	mm
internal pipe diameter	di	mm
external pipe diameter	de	mm
number of pipes	nb	null
liquid maximum flow c...	1	null
gas maximum flow coe...	1	null
equivalent emission fac...	0.05	null

b

Title	Value	Unit
@ shaft speed	1000	rev/min

d

Title	Value	Unit
solid type index	1	
material definition	pure copper (Cu)	

f

h

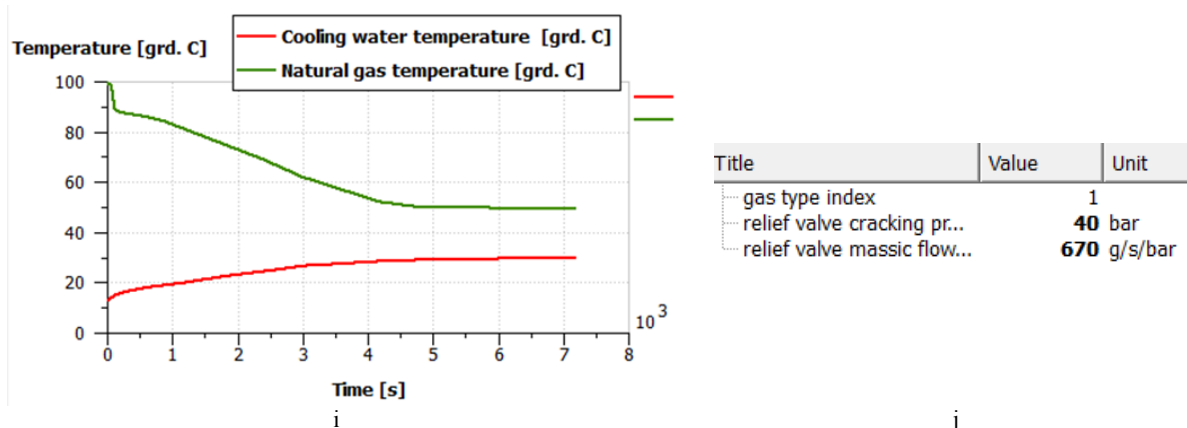


Figure 6. Modeling of the the gas cooling system in the final heat exchangers: a. gas composition modeling; b. heat exchanger parameters; c. cooling pump displacement; d. engine speed operating the cooling pump; e. cooling water characteristics; f. material for the pipes of heat exchanger; g. choosing the characteristics for the methane component from the program library; h. choosing the characteristics for the ethane component from the program library; i. temperature variation for coolant and gas on the final heat exchanger (at the outlet); j. parameters of the gas circuit discharge valve.

2.3. Reciprocating compressor cooling model

The problem of piston compressor cooling is analysed in numerous works, by different methods [17-23]. In this paragraph the cooling system is modelled in the LMS Amesim program. The cooling modelling of the gas in the final heat exchanger of the compressor is done with the help of the numerical model shown in fig. 1.a. For gas, the model described by the Gas Mixture instrument was used, which includes the components of natural gas. These can be seen on the left side of fig. 1.a. Each component receives a serial number fig. 6.a and the molar fractions for each of them are specified. The model presented is extremely detailed including most of the elements of the real system (143 variables). Thus are introduced the characteristics of the heat exchanger fig. 6.b. For the pump that circulates the water from the cooling circuit we have: the displacement of the cooling pump fig. 6.c; engine speed operating the cooling pump fig. 6.d; the characteristics of the cooling water fig. 6.e. The parameters of the gas circuit discharge valve are in fig. 6.j. The material for the pipes of heat exchanger is chosen from the library of the program fig. 6.f. The choice of the characteristics for the natural gas components from the program library is analogous: the choice of the characteristics for the methane component fig. 6.g; choosing the characteristics for the ethane component from the program library fig. 6.h; likewise, the choice is made for the rest of the components.

2.4. Cooling model results

The temperature variation for the coolant and for the gas on the heat exchanger can be seen in fig. 6.i. It is observed that on this exchanger a thermal gradient of 51 °C is ensured on the gas circuit. A thermal gradient of 17 °C is obtained on the cooling water circuit.

3. Conclusions

Using a dynamic model gives the following advantages: simplifies the mathematical aspect using the elements from the program library; shortens the realization time of the model; it allows to obtain a model that takes into account: gas composition, geometric elements of compression cylinders including dead space, compressibility of the gas on the suction / discharge pipe, variation of the pressure on the suction and discharge of the compressor, settings of the speed, dead space, valve locking in the open position; it can be easily adapted to changes in order to use an acoustic filter.

For the case exemplified in the point 2.2 the conditions imposed by the API 618 standard for the pressure variation are met for the suction area: the effective pressure variation 0.08 bar is less than the limits imposed on the pipeline flange and the compressor flange 0.1 bar and 0.28 bar respectively.

For the discharge area the condition imposed by the standard is met only at the compressor flange: the effective variation of the pressure 0.50 bar is less than the imposed limit 0.84 bar. At the pipe flange the pressure variation of 0.5 bar is above the imposed limit of 0.22 bar.

Adjusting the compressor by removing the suction valve increases the pressure variation from 0.5 bar to 0.8 bar. Increasing the dead space from 12% to 24% increases the pressure variation from 0.5 bar to 0.79 bar.

Although the solution with an acoustic filter leads to additional energy consumption, it can be applied because it ensures smaller pressure variations and we can meet the conditions specified at the flange of the discharge pipe. In this case the dimensioning of the choke is important because in a 30 mm choke diameter, with a length of 1 m we can have a pressure drop on the choke of 0.75 bar (an additional energy consumption of 45,936 kWh / year) and in a choke of 50 mm diameter with a length of 2 m we have a pressure drop of 0.12 bar additional energy consumption 5,918 kWh / year.

We can also stop the transmission of vibrations over the cutoff frequency of the filter; for example on the last line of table 1, vibrations frequencies above 5.21 Hz are not transmitted to the piping system. Heat exchange problems can be easily studied using the tools in the program for the heat exchanger, pipes and cooling system. For the case exemplified in point 2.3, a thermal gradient on the natural gas circuit of 51 °C is provided for a cooling water flow of 450 lpm, the cooling water being heated with 17 °C. Changes can be made easily (for example to the flow rate of the cooling fluid and the inlet temperature of this fluid in the heat exchanger) and the effects on the thermal gradients can be seen quickly in accordance with the technological requirements of the compression system.

References

- [1] API Standard **618** 2007
- [2] Howes B and Greenfield S 2002 *4th Int. Pipeline Conference Calgary Canada IPC'02* pp 1-10
- [3] Atkins K et al 2004 *Gas Machinery Conf. in Albuquerque New Mexico GMRC 2004* pp 1-22
- [4] Ghanbariannaeni A et al 2016 *J Process Mechanical Eng.* **230** (1) pp 65–75
- [5] Watchel J C and Tison J D 1996 *Fifth International Conference on Process Plant Reliability, Houston Texas, October 2-4* pp 243-271
- [6] Shejal P and Desai A D 2014 *Int. J Modern Engineering Research (IJMER)* **4** (7) pp 1-23
- [7] Zhao Y et al 2017 *Hindawi Shock and Vibration* 2017 pp 1-12
- [8] Jia X et al 2014 *J Vibration and Acoustics* **136** pp 98-105
- [9] Almasi A 2009 *World Academy of Science Engineering and Technology* **55** pp 321-329
- [10] Okasha A et al 2016 *J Applied Acoustics* **109** pp 44-53
- [11] Liu Z et al 2017 *J Mechanical Engineering Science* **231**(3) pp 473–484
- [12] Almasi A 2009 *J. Process Mechanical Engineering* **224** pp 63-66
- [13] Liu Z et al 2017 *J Process Mechanical Engineering* **231**(3) pp 600–612
- [14] Liu Z and Feng Q 2016 *J Power and Energy* **230** (1) pp 99–111
- [15] Fifer F 1994 *73rd Annual GPA Convention New Orleans* pp 1-6
- [16] Belman-Flores J M 2015 *Int. J of Refrigeration* **59** pp 144–156
- [17] Yinshui L et al 2019 *Int. J. of Refrigeration* **97** pp 169-179
- [18] Yusha V L et al 2016 *Procedia Engineering* **152** pp 297 – 302
- [19] Yusha V L et al 2015 *Procedia Engineering* **113** pp 264 – 269
- [20] Tuhovcak J et al 2016 *Applied Thermal Engineering* **103** pp 607-615
- [21] Balduzzi F et al 2014 *Proceedings of the ASME 2014 Pressure Vessels & Piping Conference PVP2014 July 20-24 Anaheim California USA* 28702
- [22] Pereira E et al 2012 *International Compressor Engineering Conference* 2086
- [23] Xin R and Hatzikazakis P 2000 *Int. Compressor Engineering Conference* 1360
- [24] Pana I 2007 *Hydrocarbon transport and storage systems* (Ploiesti: Petroleum and Gas University Publishing House) pp 86